Biochimica et Biophysica Acta 1788 (2009) 587–599

Contents lists available at ScienceDirect

Biochimica et Biophysica Acta

journal homepage: www.elsevier.com/locate/bbamem

Expression of sarco/endoplasmic reticulum Ca^{2+} ATPase (SERCA) 3 proteins in two major conformational states in native human cell membranes

Elisabeth Corvazier [a,1], Raymonde Bredoux [a,1], Tünde Kovács [b], Jocelyne Enouf [a,*]

[a] INSERM U 689, CRCIL, Hôpital Lariboisière, 41, Boulevard de la Chapelle, 75475 Paris Cedex 10, France
[b] Membrane Research Group, Hungarian Academy of Sciences, Dioszegi u. 64, H-1113 Budapest, Hungary

ARTICLE INFO

Article history:
Received 24 June 2008
Received in revised form 29 November 2008
Accepted 5 December 2008
Available online 16 December 2008

Keywords:
Ca^{2+}
Sarco/endoplasmic reticulum Ca^{2+} ATPase
SERCA3
Isoform
Proteolysis trypsin
Site-directed mutagenesis
Platelet
HEK-293 cell
TG
tBHQ

ABSTRACT

The SERCA family includes 3 genes (*SERCA1–3*), each of which giving rise to various isoforms. To date, detailed structural data is only available for the SERCA1a isoform. Here, limited trypsinolysis of either human platelet membranes or recombinant SERCA3a in HEK-293 cells followed by Western blotting using antibodies covering different regions of the SERCA3(a) protein revealed two, kinetically distinct, *E*arly (*ETF*) and *L*ate (*LTF*) *T*ryptic *F*ragmentations. The ETF uses many tryptic sites while the LTF uses a unique tryptic site. Using site-directed mutagenesis: i) Arg^{334}, Arg^{396} and Arg^{638} were directly assigned to the ETF and ii) Arg^{198} was assigned as the only tryptic site to the LTF. Arg^{671}, Lys^{712}/Lys^{713} and Lys^{728} were also found to modulate the ETF. SERCA inhibitors Tg and tBHQ induced modest inhibition of the ETF. In contrast, the addition of $CaCl_2$, EGTA or AlF_4^- strikingly modified the ETF without any effect on the LTF. Trypsinolysis of the other recombinant SERCA3b–3f isoforms revealed: i) same ETF and LTF as SERCA3a, with variations of the length of the C-terminal fragments; ii) Arg^{1002} as an additional tryptic site in SERCA3b–3e isoforms. Taken together, the two distinct SERCA3 fragmentation profiles sign the co-expression of SERCA3 proteins in two conformational states in cell membranes.

1. Introduction

The sarco(endo)plasmic reticulum Ca^{2+} ATPases (SERCAs) transport Ca^{2+} against an electrochemical gradient from the cytoplasm into the intracellular membranous compartment of the sarcoplasmic or endoplasmic reticulum and play a major role in Ca^{2+} homeostasis in both muscle and non-muscle cells. SERCA proteins are encoded by a multigenic family that includes 3 (*ATP2A1–3*) genes. Each gene gives rise to alternatively spliced isoforms. Until recently, *SERCA1* and *SERCA2* genes were known to generate two isoforms, which differ in their C-termini. They are mainly expressed in adult (SERCA1a) and neonatal (SERCA1b) skeletal muscles, in cardiac muscle (SERCA2a) and in all cell types (SERCA2b). Very recently, we described a new human SERCA2c isoform [1]. The third gene, *SERCA3*, was also recently shown to have various 3′-end splice variants encoding species-specific isoforms with different C-termini, including 5 SERCA3b–3f variants in humans, 2 SERCA3b–3c in mice and 1 SERCA3b/c in rats, in addition to the species-unspecific SERCA3a isoform [2].

The ion-translocation cycle of SERCAs is conventionally explained by the *E*1/*E*2 theory, where *E*1 and *E*2 refer to the high and low Ca^{2+}-affinity states, respectively. Gating of the ion pathway is coupled to autophosphorylation and dephosphorylation of the Ca^{2+} pump. Phosphoryl transfer from ATP to an Asp in the cytoplasmic domain (i.e., $E1.2Ca^{2+} \rightarrow E1P$) closes the cytoplasmic gate, and the release of ADP triggers a change in the affinity of the Ca^{2+} binding sites ($E1P \rightarrow E2P$) and the opening of the luminal gate. Hydrolysis of the aspartylphosphate ($E2P \rightarrow E2$) closes the gate. X-ray crystallography of SERCA1a has established that along with a transmembrane domain, this pump consists of three cytoplasmic domains (A, actuator, P, phosphorylation and N, nucleotide binding) that undergo very large domain movements during the reaction cycle. Recent progress in crystallography has yielded high-resolution structures from SERCA1a in various conformations [3–6]. However, crystals of proteins are usually obtained under conditions that may differ from physiological conditions. In addition, these findings concern the SERCA1a isoform, exclusively. Consequently, no structural data is available on SERCA3. A study of *SERCA3* gene products is of interest for a number of reasons (see Discussion). Of note, early studies revealed a number of functional particularities of SERCA3a in the SERCA family including its lower

Abbreviations: SERCA, sarco/endoplasmic reticulum Ca^{2+} ATPase; *E*2 and *E*1, nonphosphorylated forms of Ca^{2+} ATPase; Tg, thapsigargin; tBHQ, 2,5-di-*tert*-butyl-1,4-benzohydroquinone; HEK, human embryonic kidney; ETF, Early Tryptic fragmentation; LTF, Late Tryptic fragmentation; aa, amino acid

* Corresponding author. Tel.: +33 01 53 21 67 77; fax: +33 01 53 21 67 39.
E-mail address: jocelyne.enouf@inserm.fr (J. Enouf).

[1] Both authors contributed equally to this work.

0005-2736/$ – see front matter © 2008 Elsevier B.V. All rights reserved.
doi:10.1016/j.bbamem.2008.12.004

affinity towards Ca^{2+} than that observed for the SERCA1a, -2a and -2b proteins [7]. This lower Ca^{2+} affinity of SERCA3a was somewhat unexpected. Among the explanations, it was proposed that the reduced Ca^{2+} affinity of SERCA3a might reflect an alteration in the *E*1 to *E*2 equilibrium during the ion translocation by this enzyme.

Of a potential interest, in an earlier study, analysis of acylphosphate intermediate (E~P) formation and the PL/IM430 antibody (raised against *PL*atelet *I*ntracellular *M*embranes) recognition of platelet Ca^{2+} ATPases and their proteolytic fragments upon trypsinolysis, revealed two tryptic fragmentation patterns of the so-called 97-kDa SERCA, identified later as SERCA3a [8]. The first pattern resulted in the formation of a 73/68-kDa intermediary doublet fragment and, on a second tryptic cleavage, the production of a 40-kDa fragment previously unknown in the SERCA family. All of these were immunostained by the PL/IM430 antibody. In a later work, by performing an immunoprecipitation using a PL/IM430-affinity matrix in combination with the N89 anti-SERCA3 antibody [9], we documented that the epitope for the PL/IM430 antibody could be localized in the SERCA3-related N-terminal 40-kDa tryptic fragment [10]. However, the relevance to SERCA3 of the PL/IM430-recognizable fragments could only be definitely established when the epitope of the antibody was determined. Chandrasekera et al. demonstrated that PL/IM430 antibody is a pan-SERCA3 antibody that binds to the so-called actuator (A) domain, which comprises a tightly folded independent structure containing aa 1–40 and 126–230 of SERCA3 [11]. The second tryptic fragmentation pattern of the 97-kDa SERCA resulted in the late production of an E~P-forming 80-kDa fragment not recognized by PL/IM430. Initially detected by different groups using trypsinolysis of native platelet membranes [8,12–15], this 80-kDa fragment was recovered later on through trypsinolysis of recombinant human SERCA3a protein [9]. Subsequently, progress in the structure of SERCA1a [3–6] showed that the accessibility of the T2 tryptic site (Arg^{198}) that gives rise to a fragment of similar MW depended on the SERCA1a conformational state.

In the present work, we aim to identify these two tryptic fragmentation profiles as the ones coming from two conformational states of SERCA3. We approached this issue primarily by performing trypsin-induced proteolysis coupled with site-directed mutagenesis experiments that appeared to be a successful approach during structural/functional studies of the SERCA1a isoform [16–18].

2. Materials and methods

2.1. Platelets

Human blood was obtained from healthy volunteers and the investigation was performed according to the requirements of the Helsinki Declaration. The platelets were isolated as described previously [19].

2.2. Cell culture

A human embryonic kidney (HEK-293) cell line was obtained from the American Type Culture Collection (Manassas, VA). Cells were grown in RPMI 1640 medium with Glutamax-I, supplemented with 10% heat-inactivated fetal calf serum, 100 U/ml penicillin and 100 μg/ml streptomycin.

2.3. Stable and transient transfection in HEK-293 cells

cDNAs for transfection were purified using a plasmid purification kit (Macherey-Nagel, Düren, Germany). Cells were transfected with 10 μg of the cDNAs using the transfection agent ExGen 500 (Euromedex, Souffelweyersheim, France). Stable transfections have been described previously [20,21]. For transient transfections, cells were cultured for 48 h.

2.4. Construction of SERCA3 mutants

Mutations were generated by site-directed mutagenesis of SERCA3a/pcDNA3, SERCA3b/pcDNA3 or SERCA3e/pcDNA3 constructs, using Quick Change XL Site-directed Mutagenesis Kit from Stratagene (La Jolla, CA, USA). Several point mutations giving switch amino acids were performed: Arg^{198}→Ala; Arg^{334}→Ala; Arg^{396}→Ala; Arg^{638}→Ala; Arg^{671}→His; Lys^{712}→Ala; Lys^{713}→Ala; Lys^{728}→Ala for SERCA3a and Arg^{1002}→Ala for SERCA3b and SERCA3e. A number of double mutants were also obtained, including Arg^{334}/Arg^{396}→Ala^{334}/Ala^{396}; Arg^{334}/Arg^{638}→Ala^{334}/Ala^{638}; and Lys^{712}/Lys^{713}→Ala^{712}/Ala^{713}. However, the double mutant Ala^{334}/Ala^{396} only gave limited quantities of proteins. All the SERCA3 mutants were checked by DNA sequencing (Genome Express, France).

2.5. Preparation of platelet and HEK-293 cell membrane vesicles

Platelet membrane vesicles were isolated as described in [8]. As concerns the HEK-293 cell membrane vesicles, the cells were harvested, washed with PBS (pH 7.4) and resuspended in an ice-cold buffer containing 10 mM KCl, 10 mM K-Hepes (pH 7.0), 50 μM EGTA, 50 μM EDTA, 50 μM phenylmethylsulfonyl fluoride, 100 μg/ml soybean trypsin inhibitor, 100 μg/ml Bowman-Birk trypsin-chymotrypsin inhibitor, 100 μg/ml aprotinin and 0.1 mM dithiothreitol (DTT). The cell suspension was homogenized in a Teflon-glass homogenizer and then sonicated on ice. The lysate was centrifuged at 120 ×g for 10 min at 4 °C and the supernatant was centrifuged at 100 000 ×g for 1 h. The pellet was resuspended in a buffer containing 160 mM KCl, 17 mM K-Hepes (pH 7.0) and 0.1 mM DTT, frozen and maintained at −80 °C.

2.6. Controlled proteolysis of membrane vesicles

Trypsin treatment of membrane vesicles was carried out in proteolysis medium containing 160 mM KCl, 17 mM K-Hepes (pH 7.0), 0.1 mM DTT, 0.05 mM $CaCl_2$ and 0.1 mg/ml membrane proteins, as well as either 10 μg or 50 μg/ml trypsin for different time periods. The reaction was stopped with a 10-fold excess (w/w) of soybean trypsin inhibitor, as in [8].

2.7. Thapsigargin (Tg) and 2,5-di-(t-butyl)-1,4-benzohydroquinone (tBHQ) treatment

Membrane vesicles were treated with either 5 μM Tg or 10 μM tBHQ for 5 min at 37 °C, and subsequently placed on ice for an additional 10 min. Trypsin proteolysis was then performed as described above.

2.8. Ca^{2+}, EGTA and AlF_4^- treatments

For Ca^{2+} and EGTA treatments, membrane vesicles were incubated in a buffer containing 160 mM KCl, 17 mM K-Hepes (pH 7.0), 0.1 mM DTT and either 2 mM $CaCl_2$ or 2 mM EGTA, respectively, for 2 min at room temperature before trypsinolysis. For AlF_4^- treatment [22], membrane vesicles were incubated in a buffer containing 100 mM K-MOPS (pH 7.2), 100 mM KCl, 1 mM $MgCl_2$, and 50 μM AlF_4^- (20 μl of 5 mM $AlCl_3$ and 200 μl of 20 mM NaF) for 20 min at room temperature. After incubation, the buffer was removed by centrifugation at 10 000 ×g. The pellet was resuspended in a buffer containing 100 mM K-MOPS and 3 mM EGTA to eliminate all unbound fluoride and aluminium. After centrifugation at 10 000 ×g, the pellet was resuspended in a buffer containing 160 mM KCl, 17 mM K-Hepes (pH 7.0) and 0.1 mM DTT before trypsinolysis.

2.9. Antibodies

For SERCA2b, the pan-anti-SERCA2 monoclonal antibody IID8 was used. All SERCA3 proteins were visualized using the polyclonal N89 (PAI-

910, Affinity BioReagents, Neshanic Station, NJ), the monoclonal PL/IM430 (generous gift from Pr N. Crawford) [11] and the monoclonal ATP2A3 (Abnova, Taiwan, Republic of China) pan-anti-SERCA3 antibodies. Isoform-specific polyclonal antibodies against the SERCA3a–3d and -3f proteins were also used [10,21,23]. Secondary anti-rabbit and anti-mouse horseradish peroxidase-conjugated antibodies for immunoblottings came from Jackson Immunoresearch (West Grove, PA, USA).

2.10. Generation and characterization of a novel human SERCA3e-specific polyclonal antibody

A SERCA3e-specific polyclonal antibody was generated by immunizing SPF rabbits with a mixture of the P1 and P2 peptides, as indicated in Fig. 7A (Eurogentec, Herstal, Belgium). Eurogentec also performed the affinity purification of antiserum using each peptide. Purified anti-SERCA3e-P1 and anti-SERCA3e-P2 antibodies were tested by immunoblotting using recombinant SERCA3e protein (data not shown). The purified anti-SERCA3e-P2 antibody presented the highest immunoreactivity and was used for all immunoblotting experiments within the present study.

2.11. Electrophoresis of proteins and Western blotting

Protein electrophoresis was performed using either 7.5% acidic SDS-PAGE for the analysis of phosphoenzyme intermediate formation of SERCA3 isoforms or 10% SDS-PAGE for Western blotting of intact and proteolyzed SERCA3 proteins. After electrophoresis, the separated proteins were transferred onto nitrocellulose membranes. For Western blotting of SERCA3 proteins, nitrocellulose membranes were incubated with a 1:1000 dilution of N89, 1 μg/ml of PL/IM430, a 1:1000 dilution of ATP2A3 or a 1:1000 dilution of each of the isoform-specific antibodies against SERCA3a–3f, in Tris-buffered saline (10 mM Tris/HCl and

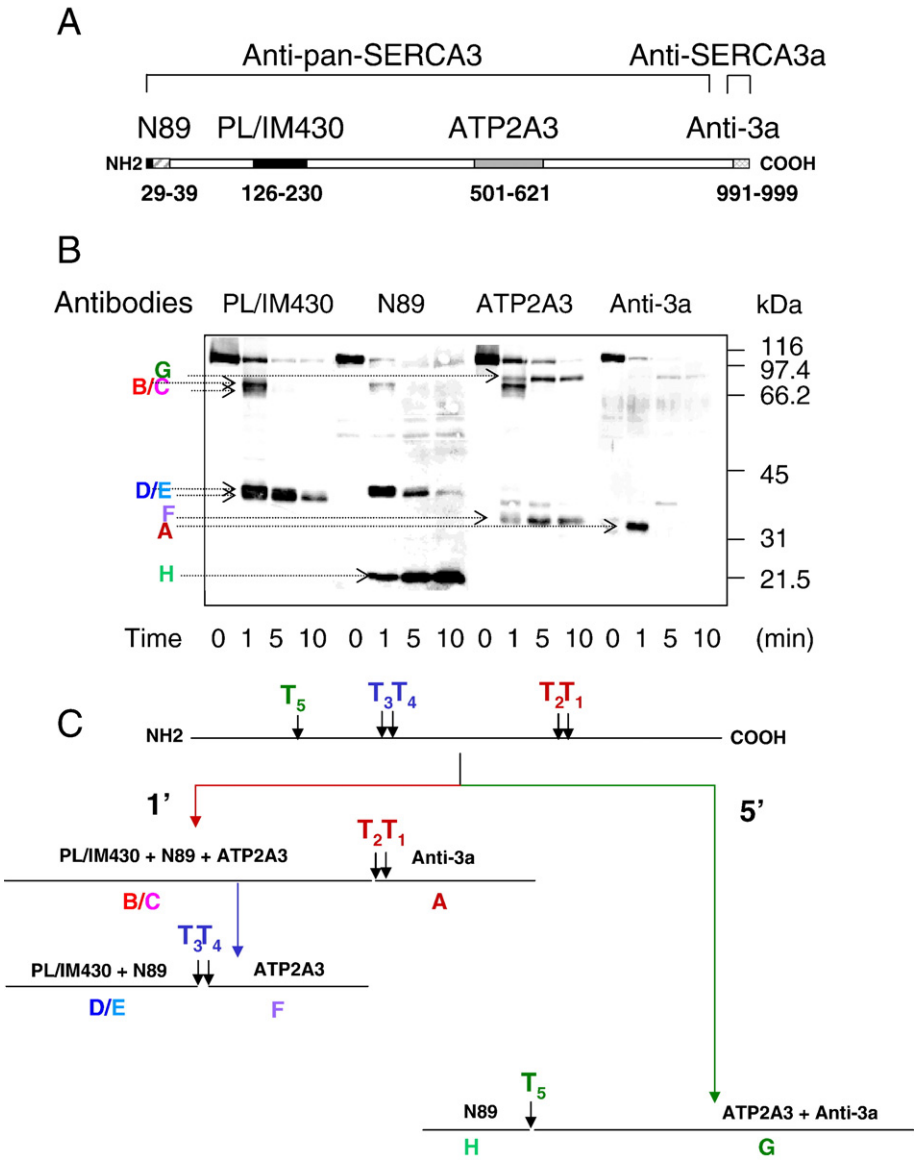

Fig. 1. Demonstration of two tryptic profiles of SERCA3a protein in human platelets. (A) Location of the epitopes of the anti-SERCA3 antibodies. Polyclonal N89, monoclonal PL/IM430, monoclonal ATP2A3 and polyclonal isoform-specific anti-SERCA3a (Anti-3a) antibodies recognize aa 29–39, 1–40 and 126–230, 501–621 and 991–999, respectively. (B) Platelet membrane vesicles (0.1 mg/ml) were proteolyzed using 50 μg/ml trypsin at 4 °C for the time periods indicated. The intact (0) and trypsin-proteolyzed Ca^{2+} ATPases were then resolved by electrophoresis on 10% SDS-PAGE (50 μg of membrane proteins/lane), blotted onto nitrocellulose membranes, and immunostained using the antibodies indicated. Tryptic fragments A to H are positioned on the left-hand side. In this and the following figures, the molecular weight markers in kDa are located on the right-hand side. (C) Schematic representation of the accessibility of tryptic sites at 1 and 5 min of trypsin proteolysis of platelet SERCA3a protein. This figure is typical of 4 experiments.

150 mM NaCl, pH 7.4), 5% (w/v) non-fat milk and 0.1% Tween 20 for 2 h at room temperature. After washing, blots were treated with a 1:10 000 dilution of horseradish peroxidase-conjugated anti-rabbit IgG (N89 and anti-SERCA3a–3f) or a 1:2000 dilution of horseradish peroxidase-conjugated anti-mouse IgG (IID8, ATP2A3 and PL/IM430). Antibody binding was revealed using enhanced chemiluminescence Western blotting reagents, as per the manufacturer's instructions. Luminograms were quantified using the Fuji LAS 3000 luminescent Image Analyzer and Multi-Gauge software (FujiFilm, Japan).

2.12. Phosphoenzyme intermediate of intact and proteolyzed SERCA3 isoforms

Phosphorylation of SERCA3 enzymes with [γ-^{32}P]ATP (0.05 μM final concentration) was carried out for 1 min at 4 °C in the proteolysis medium, immediately after proteolytic digestion, as described earlier [8,15]. The reaction was stopped by adding trichloroacetic acid (6%) solution containing phosphoric acid (10 mM) and ATP (1 mM). The precipitates were then washed three times with the same solution and finally dissolved in the electrophoresis sample buffer [8].

2.13. Calculation of the molecular weight (MW) of the tryptic fragments

For this, the ratio between the MW in kDa of the SERCA3a–3f isoforms and their number of aa was calculated. The mean value of 1 kDa for 9.15 aa was obtained. The aa (s) identified on the basis of the effect of their mutations on the tryptic profiles were used to calculate the length of the fragments in aa and their resulting MW.

Data in the present work relate to at least three independent experiments and are presented mainly in the form of representative experiments.

3. Results

3.1. Co-expression of two SERCA3a conformational states in human platelets

For this, we performed tryptic digestion of platelet membranes mainly expressing SERCA3a [10], followed by Western blotting using antibodies recognizing the N-terminal (N89) [9] and (PL/IM430) [11], middle (ATP2A3) and C-terminal (Anti-3a) [10] parts of SERCA3a protein (Fig. 1A). Fig. 1B and C show the time course of trypsinolysis using 50 μg/ml trypsin at 4 °C for the time periods indicated allowing the dissociation of two distinct *Early* (1 min) and *Late* (5 to 10 min), *Tryptic Fragmentations* of SERCA3a. They are named ETF and LTF, respectively, in the following. At 1 min, the parent B/C (73/68-kDa) and D/E (40-kDa) fragments resulting from T1/T2 and T3/T4 tryptic sites, respectively, were detected by both PL/IM430 and N89 antibodies, establishing that they belong to the N-terminal part of SERCA3a. A complementary C-terminal A (32-kDa) fragment of the B/C fragments resulting from T1/T2 trypsin attack was detected by the Anti-3a antibody. The B/C and an additional F (33-kDa) fragments were recognized by ATP2A3 antibody. This intermediate F fragment comes from the B/C fragments as a result of trypsin attack at T3/T4 tryptic sites.

Later on, i.e. at 5 to 10 min, the disappearance of these fragments was accompanied by the appearance of a second tryptic fragmentation pattern (LTF), giving rise to C-terminal G (80-kDa) and N-terminal H (22-kDa) fragments recognized by both Anti-3a and ATP2A3, and N89 antibodies, respectively. Obviously, the G fragment, longer than the longest B/C fragments of ETF, could not belong to the ETF. Therefore, these fragments were issued from another single trypsin attack at T5 site.

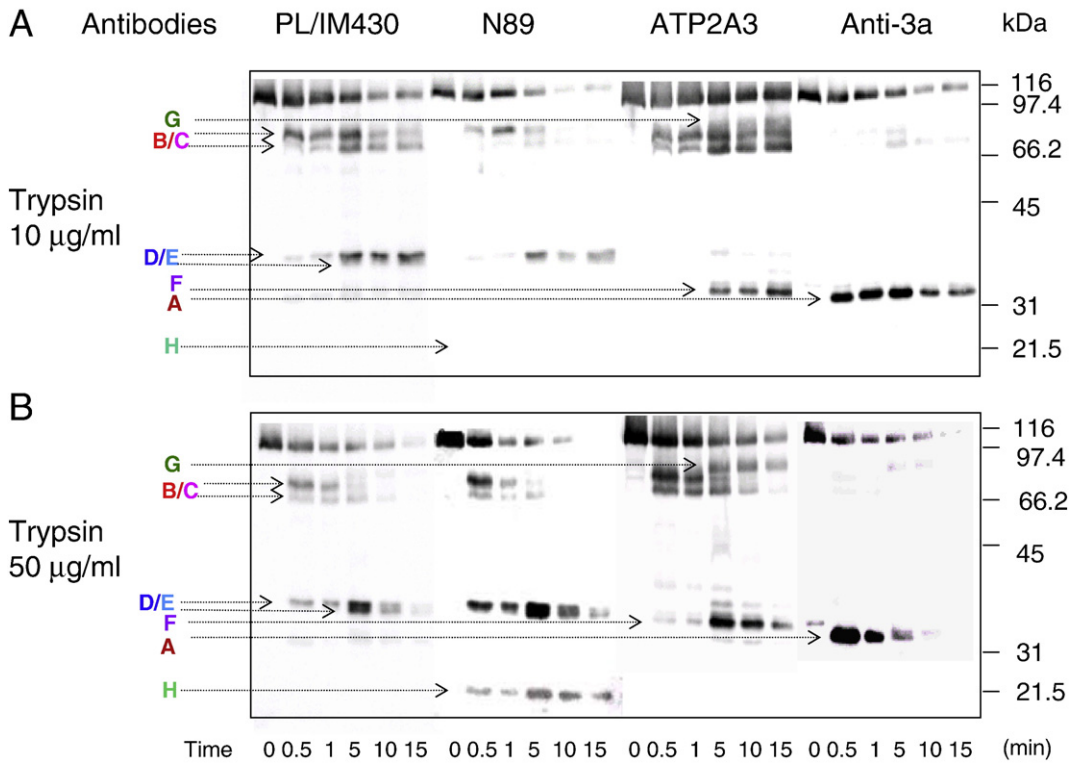

Fig. 2. Demonstration of two tryptic profiles of stable recombinant human SERCA3a protein: time-course and dose–response effects of trypsin. SERCA3a protein was stably transfected in HEK-293 cells. HEK-293 cell membrane vesicles (0.1 mg/ml) were proteolyzed using either 10 (A) or 50 μg/ml (B) trypsin at 4 °C for the time periods indicated. The intact and trypsin-proteolyzed SERCA3a proteins were then treated for Western blotting and are presented as in Fig. 1. This figure is typical of 4 experiments on the effect of both 10 μg/ml and 50 μg/ml trypsin.

Table 1

Arg residues						Lys residues		
aa	SERCA1a	SERCA3a	aa	SERCA1a	SERCA3a	aa	SERCA1a	SERCA3a
14	–	+	502	–	+	47	+	+
33	–	+	505	+	–	120	+	+
35	–	+	524	+	+	135	+	+
63	+	+	529	+	+	158	+	+
110	+	+	533	–	+	169	+	+
131	+	+	542	–	+	189	+	+
134	+	+	550	–	+	204	+	+
139	+	+	560	+	+	205	+	+
141	–	+	567	+	+	218	+	+
143	+	+	572	–	+	234	+	+
164	+	+	604	+	+	252	+	+
174	+	+	613	–	+	297	+	+
198	+	+	620	+	+	329	+	+
236	+	+	637	+	+	352	+	+
246	–	+	638	+	+	431	+	+
251	–	+	656	+	+	436	+	+
258	–	+	667	+	+	476	–	+
290	+	+	671	+	+	481	+	+
324	+	+	674	–	+	492	+	+
325	+	+	678	+	+	511	+	+
328	–	+	686	–	+	515	+	+
334	+	+	751	+	+	548	–	+
365	–	+	762	+	+	573	–	+
396	–	+	822	+	+	583	–	+
403	+	+	825	–	+	629	+	+
464	–	+	836	+	+	651	–	+
467	+	+	871	–	+	684	+	+
480	–	+	894	–	+	712	+	+
489	+	+	924	+	+	713	+	+
491	+	+	965	–	+	728	+	+
			989	+	+	758	+	+
						819	–	+
						875	–	+
						985	+	+

Amino acid similarity comparison.
+ : Presence - : Absence.
Black : Homology.
Red : Divergence.

3.2. Co-expression of two conformational states of stable recombinant human SERCA3a protein

To further identify the SERCA3 tryptic sites by site-directed mutagenesis, we used the recombinant human SERCA3a protein expressed in HEK-293 cells [20]. As a prerequisite, we looked for similarities with human platelets. Fig. 2 shows both a refined time course and dose response of the effect of trypsin on stable recombinant SERCA3a protein. Using 10 μg/ml trypsin for 0.5 to 15 min (Fig. 2A), one could see that at 0.5 min, the first tryptic site was the T1 site, which gave rise, to the concerted A and B fragments recognized by the Anti-3a antibody (A) and the PL/IM430, N89 or ATP2A3 antibodies (B), respectively. At 5 to 15 min proteolysis, the appearance of the C, D/E and F fragments was observed as well as a slight decrease in the level of A fragment. In this experimental setup (low trypsin concentration), G and H fragments could not be visualized. At 50 μg/ml trypsin concentration (Fig. 2B), differences appeared in the time-course of the appearance and disappearance of the fragments identified in the ETF. The A fragment appeared transiently. The B fragment disappeared at 5 min, while the intensity of the D/E doublet and F fragment was maximal at 5 min and then disappeared. The major differences reside in the apparition of G and H fragments, which appeared maximal at 5 to 15 min proteolysis. Thus, the ETF and LTF profiles of recombinant SERCA3a protein exhibited great similarities with those of human platelet SERCA3a protein.

We also tested the effect of trypsin on SERCA3a protein transiently expressed in HEK-293 cells. Similar results were observed (data not shown), thus further establishing the dissociation between the two tryptic profiles.

3.3. Prediction of tryptic sites involved in SERCA3a tryptic fragmentations

To predict tryptic sites for ETF of SERCA3a, we at first looked for sequence alignments of human SERCA1a and SERCA3a. Table 1 summarizes the Arg and Lys residues present in the two isoforms. SERCA3a contains 60 Arg versus 37 for SERCA1a. All Arg residues present in SERCA1a are found in SERCA3a except Arg^{505} (one of the two major tryptic sites, T1, in SERCA1a). About Lys residues, SERCA3a contains 34 Lys versus 27 for SERCA1a. Again, all Lys residues present in SERCA1a are found in SERCA3a. Second, we focused on findings on rabbit SERCA1a showing 3 tryptic sites known as T3 (Arg^{334}), T4 (Arg^{638} or Arg^{639}) and T5 (Lys^{728}) when skeletal muscle sarcoplasmic reticulum membranes were extracted in the presence of EDTA before trypsinization [24]. These tryptic fragments of SERCA1a could display similarities with the B/C and D/E fragments of SERCA3a. Third, some preliminary assays for the modeling of the structures of SERCA3 in *E*1 and *E*2 conformations (personal data, Pr J.T. Penniston, Massachusetts General Hospital, Boston, USA) suggested different accessibility for Arg^{396} and Arg^{403} in the two conformational states. Fourth, the approximate locations of either Arg or Lys residues, as a function of the estimated MW of the fragments of ETF, were also tested with the inclusion of Arg^{671} and Lys^{712}/Lys^{713}. Last, to predict the cleavage site for LTF, we were helped by previous data suggesting the identity of the T5 tryptic site (Fig. 1C) with the T2 tryptic site of SERCA1a [9].

3.4. Identification of Arg^{334} and Arg^{396} as candidate tryptic sites in early tryptic fragmentation

Fig. 3 shows the results of the effects of 50 μg/ml trypsin for 1 to 5 min on transiently transfected Wild Type SERCA3a (WT) and its

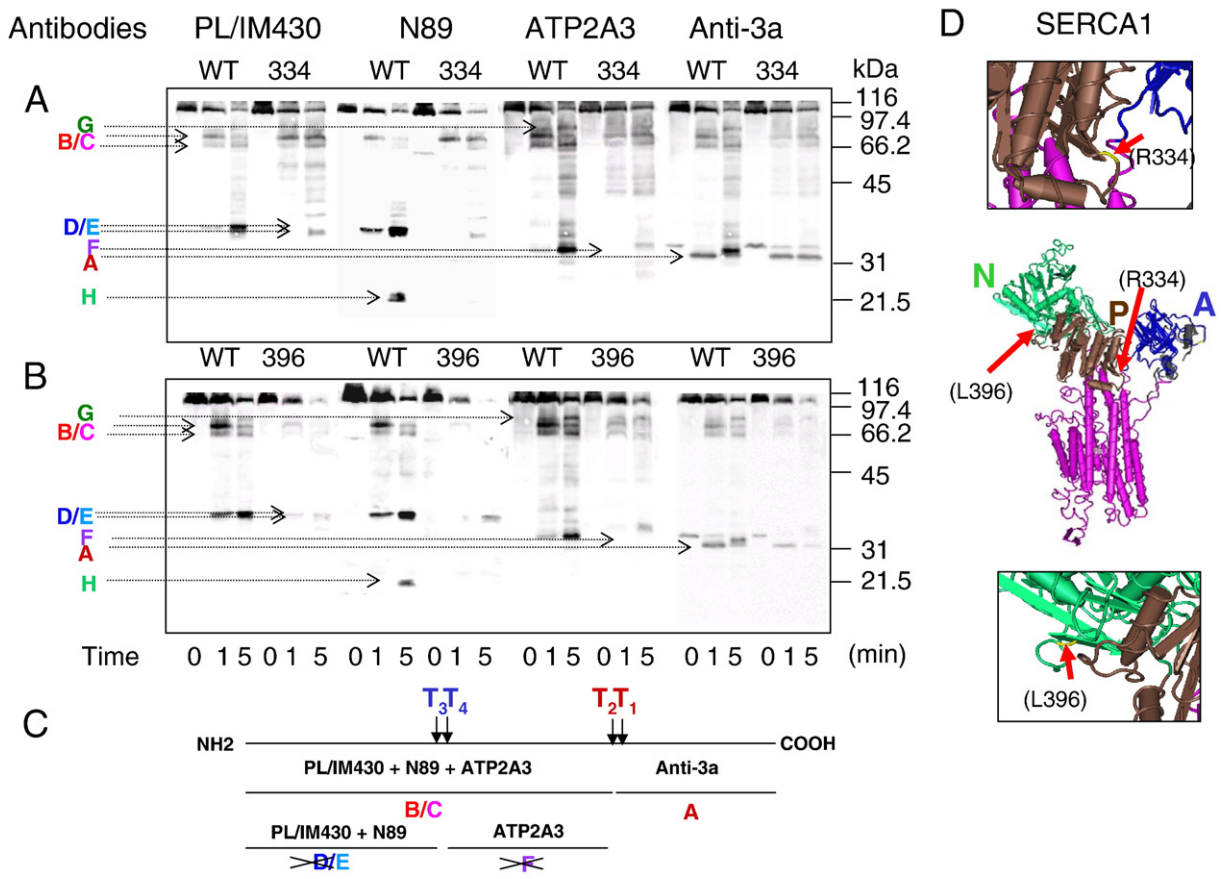

Fig. 3. Involvement of Arg^{334} and Arg^{396} in early tryptic fragmentation. Recombinant SERCA3a protein was mutated at either Arg^{334} or Arg^{396}. Mutated proteins were transiently transfected in HEK-293 cells and membrane vesicles were proteolyzed using 50 μg/ml trypsin for the time periods indicated. The intact and trypsin-proteolyzed Wild Type (WT) and R334A (334) or R396A (396) mutated SERCA3a proteins were then treated for Western blotting as in Fig. 1. (A) Effect of R334A mutation; (B) Effect of R396A mutation; (C) Schematic representation of the effect of both R334A and R396A mutations on tryptic fragmentation. This figure is typical of 5–7 experiments. (D) Based on the sequence similarity of SERCA3a with SERCA1a, the trypsin cleavage sites (in yellow) of SERCA3a are mapped on the atomic model of SERCA1a in the E1 state (Protein Data Bank code 1su4). R334 (R334 in SERCA3a) and L396 (R396 in SERCA3a) are shown.

R334A (Fig. 3A) or R396A (Fig. 3B) mutants. Surprisingly, with the exception of some destabilization of R396A mutant (it disappears more quickly than the WT), striking similarities appear in the mutagenesis-related changes of the tryptic profiles. These mutations were found to abolish or inhibit the second step of ETF (i.e. the fragmentation of the B/C doublet) and to markedly decrease LTF (i.e. the formation of G and H fragments). Both mutations clearly suppressed the D fragment and inhibited the E fragment of the D/E doublet as shown by both the PL/IM430 and N89 antibodies, and blocked the formation of F fragment recognized by the ATP2A3 antibody. This was consistent with the concerted apparition of D/E and F fragments in WT SERCA3a as a result of trypsin attack at T3/T4 sites. This led us to calculate the exact MW of D fragment as 36.5-kDa. As expected, trypsinolysis of these SERCA3a mutants exhibited similar A fragment. In addition, a concerted decrease in appearances of G and H fragments was observed in both mutants as shown by ATP2A3 and Anti-3a antibodies for G fragment and N89 antibody for H fragment. Thus, R334A and R396A mutants were also found to inhibit the accessibility of the T5 tryptic site involved in LTF.

To understand the similarities between the effects of R334A and R396A mutations on ETF (Supplemental Fig. 1) we refined the experimental conditions of Western blotting with PL/IM430 (panel A) and ATP2A3 (panel B) antibodies. Supplemental Fig. 1A establishes that the proteolysis of the two mutants shows the absence of D fragment and the inhibition of the formation of E fragment (trypsin attack at Arg^{324}?). An additional I fragment was also observed. Supplemental Fig. 1B shows that the absence of F fragment was compensated by the J fragment of higher MW (trypsin attack at Arg^{290}?) in both mutants, added to a K fragment of lower MW in R334A mutant, only. This smaller fragment is obviously due to trypsin attack at Arg^{396}, as it is totally absent in R396A mutant. In addition, its lower MW is consistent with the expected difference of 6.7-kDa corresponding to the 62 aa long region between Arg^{334} and Arg^{396} tryptic sites. Thus, the tryptic profiles observed in the two mutants can be explained by the fact that R334A mutation induces the accessibility of Arg^{396} while R396A mutation prevents that of Arg^{334} (Supplemental Fig. 1C).

3.5. Identification of Arg^{638} as candidate tryptic site in early tryptic fragmentation

Fig. 4 shows the ETF profiles of R638A mutant and R334A/R638A double mutant. When using R638A mutant, the appearance of the B/C doublet was inhibited as shown by either the PL/IM430 (Fig. 4A) or the ATP2A3 (Fig. 4B) antibodies. This mutant was also found to exhibit similarities with R334A and R396A ones as concerns the disappearance of both the D and F fragments (Fig. 4A and B, respectively). Thus, the mutation of Arg^{638} abolished the accessibility of Arg^{334} (Fig. 4C). We also compared the effect of R638A mutation with that of the R334A/R638A double mutation. Interestingly, the B/C doublet was present in the ETF profile of this double mutant, may be due to a tryptic attack at Arg^{637} instead of Arg^{638}. Immunostaining with

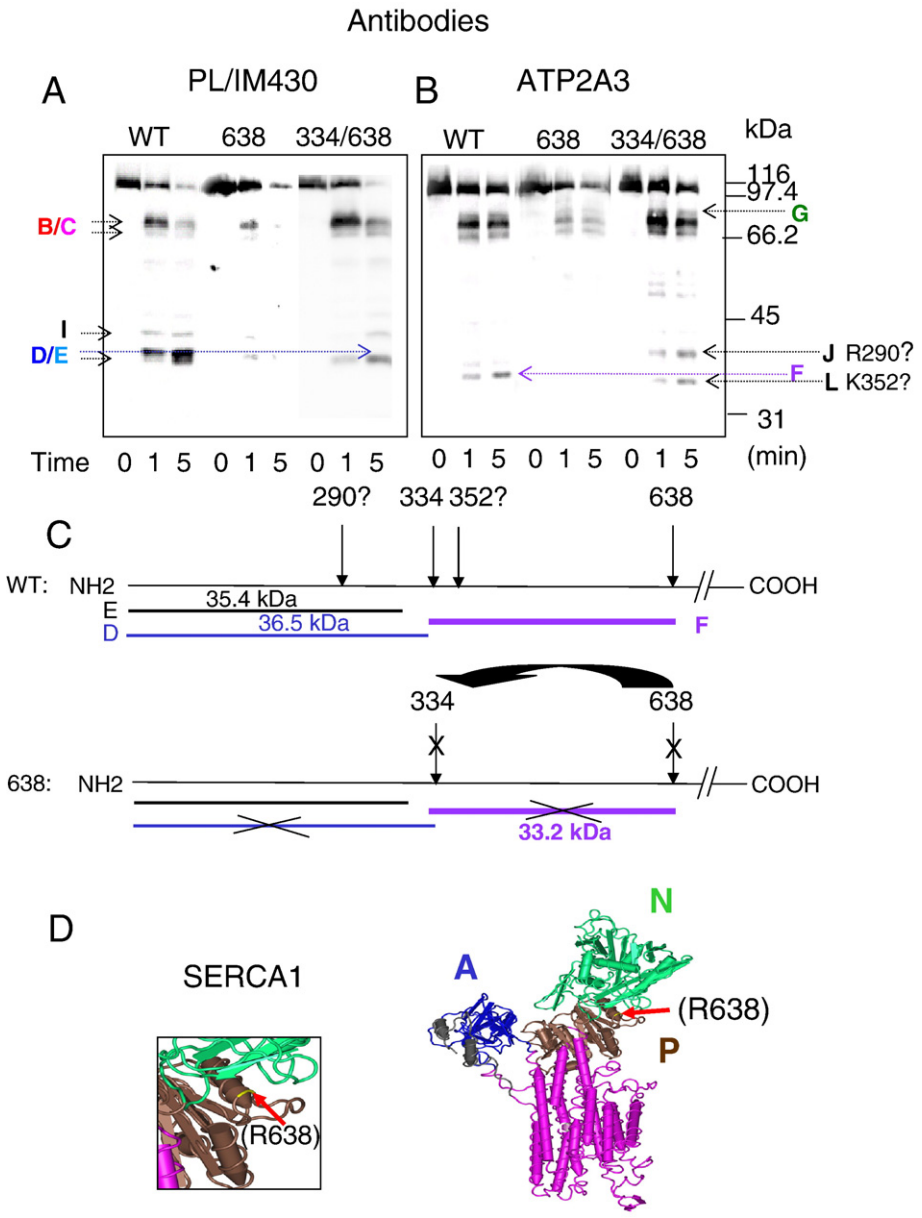

Fig. 4. Involvement of Arg^{638} in early tryptic fragmentation. (A and B) Comparative effect of the mutation of Arg^{638} and of Arg^{334}/Arg^{638} on early tryptic fragmentation induced by 50 μg/ml trypsin for the time periods indicated. WT, R638A (638) and R334A/R638A (334/638) mutated SERCA3a proteins were treated for Western blotting as in Fig. 1. (A) PL/IM430; (B) ATP2A3. (C) Schematic representation of the effect of the mutation of Arg^{638} on the accessibility of Arg^{334}. This figure is typical of 3–4 experiments. (D) In a similar manner as in Fig. 3D, R638 (R638 in SERCA3a) is shown.

ATP2A3 revealed two additional fragments J and L. According to their MW, they may refer to trypsin attack at Arg^{290} and Lys^{352}, respectively. The identification of the Arg^{638} tryptic site led us to calculate the exact MW of F fragment as 33.2 kDa.

3.6. Involvement of Arg^{671}, Lys^{712}/Lys^{713} and Lys^{728} in early tryptic fragmentation

In a further attempt to identify the T1/T2 tryptic sites, we studied the R671H, K712A/K713A and K728A mutants. While these mutants did not directly abolish the T1/T2 tryptic sites as visualized by PL/IM430 and ATP2A3 antibodies, mutants induced an increase in F and D fragments, respectively, while double mutant K712A/K713A induced a decrease in A fragment (data not shown). So, these tryptic sites may very well account for the possible multi-tryptic sites implicated in the initial C-terminal fragmentation.

3.7. Identification of Arg^{198} as tryptic site in late tryptic fragmentation

For this, we took advantage of previous works on both SERCA1a and SERCA3 proteins. SERCA1 and SERCA2 proteins present two major tryptic sites termed T1 (Arg^{505}) and T2 (Arg^{198}) [25–29]. A SERCA-related fragment of about 80-kDa had been described upon trypsin proteolysis of platelet membranes and recombinant SERCA3a protein [8,9,12–15]. It was suggested that the formation of this fragment may appear in the absence of the T1 tryptic site (Arg^{505}) of SERCA1 and SERCA2 in SERCA3 (Table 1). However, the exact identity of the tryptic site of SERCA3a, with the T2 site (Arg^{198}) of SERCA1 and SERCA2, was not demonstrated at that time. Here, by using R198A SERCA3a mutant, we clearly identified it as the T5 tryptic site that gives rise to G and H fragments (Fig. 5). R198A mutation shows that neither the C-terminal G fragment (recognized by both ATP2A3 and Anti-3a antibodies), nor the N-terminal H fragment (recognized by

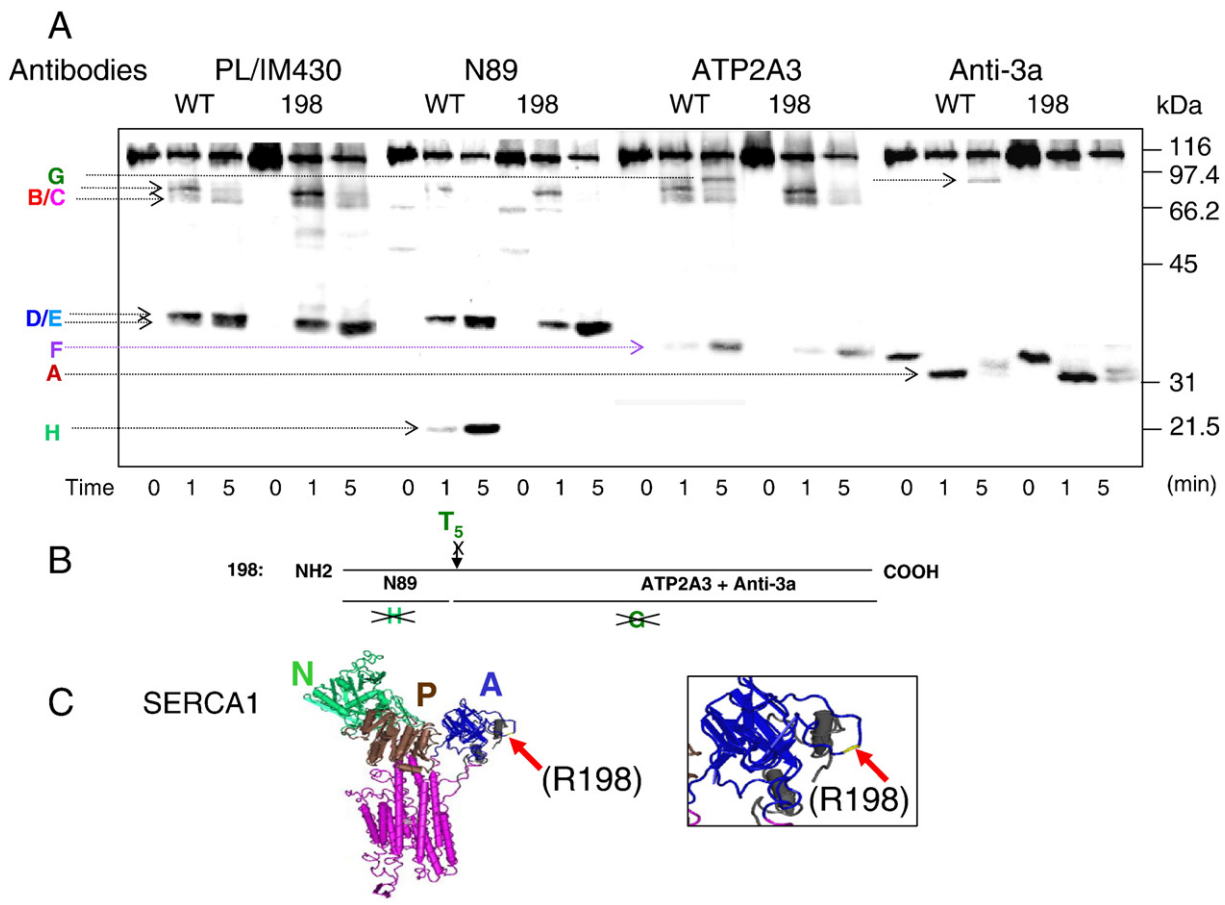

Fig. 5. Involvement of Arg^{198} in late tryptic fragmentation. (A) Recombinant SERCA3a protein was mutated at residue Arg^{198} (R198A) and transiently transfected in HEK-293 cells. Membrane vesicles were further proteolyzed using 50 μg/ml trypsin for the time periods indicated. Wild Type (WT) and mutated SERCA3a protein (Arg^{198}) were then treated for Western blotting as in Fig. 1. (B) Schematic representation of the effect of the mutation of Arg^{198}. This figure is typical of 5 experiments. (C) In a similar manner as in Figs. 3D and 4D, R198 (R198 in SERCA3a) is shown.

N89) could be detected upon trypsinolysis of this mutant. This led us to calculate that the G and H fragments exhibit exact MW of 87.5- and 21.5-kDa, respectively. In addition, and as expected, R198A mutation had no effect on the ETF of SERCA3a. This led us to think that Arg^{198} (T5 tryptic site) is hidden in the SERCA3a conformation giving rise to the ETF profile of this enzyme.

3.8. Effect of SERCA inhibitors thapsigargin (Tg) and tert-butyl benzohydroquinone (tBHQ) on tryptic fragmentation of SERCA3a

In order to further establish the two conformational states of SERCA3a, we checked whether modulation of its two tryptic fragmentation profiles occurred upon addition of 5 μM Tg (Supplemental Fig. 2) or 10 μM tBHQ (data not shown) for up to 10 min at 37 °C before trypsinolysis. These SERCA inhibitors were previously shown to induce the so-called *E2*(Tg) state of SERCA1a [4,18]. Supplemental Fig. 2 shows that Tg slightly modified the ETF, and that the modification displayed similarities with what was observed with the R334A mutant. A decrease in the recognition of the D/E doublet by the PL/IM430 and N89 antibodies was observed, due purely to the abolishment of the D fragment. This observation was associated with the disappearance of F fragment visualized by ATP2A3 antibody. As regards LTF, no major modification was observed, as both G and H fragments were still present as visualized by ATP2A3, Anti-3a and N89 antibodies, respectively. Again, no major modification of the ETF and LTF was made using 10 μM tBHQ (data not shown).

3.9. Effect of Ca^{2+}, EGTA and AlF_4^- on tryptic fragmentation of SERCA3a

In order to check whether the ETF does not reflect the presence of partially unfolded protein in our membrane preparations, we tested the effects of 2 mM $CaCl_2$, 2 mM EGTA and 50 μM AlF_4^- (a phosphate mimic [22]) on tryptic fragmentation of SERCA3a. Fig. 6 shows that Ca^{2+}, EGTA and AlF_4^- strongly affected the ETF without modifying the LTF. Moreover, differences were found according to the treatment. The addition of either $CaCl_2$ or AlF_4^- inhibited the ETF as shown by the decrease in B/C and D/E fragments seen by PL/IM430 and N89, as well as by the decrease in F fragment visualized by ATP2A3 antibody, respectively. Conversely, EGTA was found to increase the ETF as shown by the increased intensity of same D/E and F fragments. In contrast, various additions, Ca^{2+}, EGTA or AlF_4^-, did not affect the appearance of the H fragment (shown by the N89 antibody) in the LTF profile of SERCA3a.

Notes to Figure 5.
(We were also surprised by the apparent higher expression of SERCA3a in R198A mutant, detected with the PL/IM430, ATP2A3 and Anti-3a antibodies. Indeed, when verifying the amounts of proteins deposited on the gels by using Ponceau Red, we found no differences between WT and R198A mutant. Moreover, by comparing the different antibodies, one can see that differences exist between the antibodies, as for example, N89 antibody could detect almost same amounts of WT and R198A mutant. We should also take into consideration that PL/IP430 antibody is now defined as a conformational antibody [11]. In this context, we also observed that after autophosphorylation, N89 recognition of SERCA3a in platelet membrane preparations was apparently lower (unpublished data).)

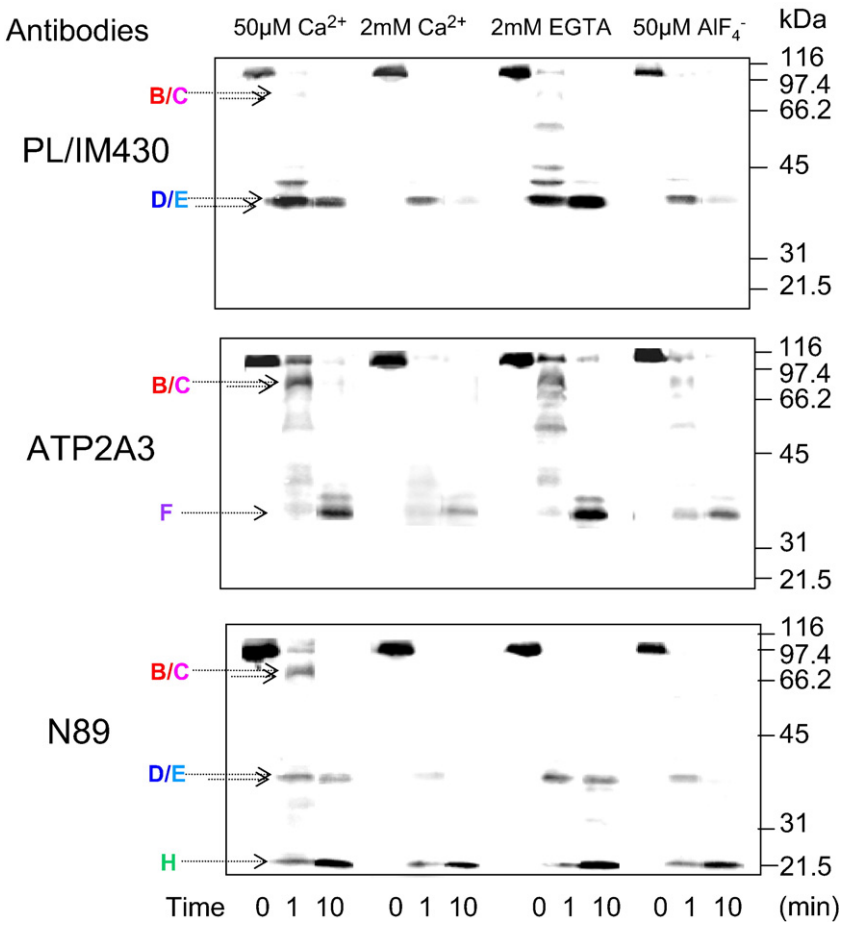

Fig. 6. Comparative effects of Ca^{2+}, EGTA and AlF_4^- on early and late tryptic profiles. Recombinant SERCA3a protein was transiently transfected in HEK-293 cells. Membrane vesicles were treated with either 2 mM $CaCl_2$, 2 mM EGTA or 50 μM AlF_4^- as described under Materials and methods. Membrane vesicles were further proteolyzed using 50 μg/ml trypsin for the time periods indicated and treated for Western blotting using the antibodies indicated. A, Untreated membrane vesicles (50 μM $CaCl_2$ in the proteolysis medium). B, Membrane vesicles treated with $CaCl_2$. C, Membrane vesicles treated with EGTA. D, Membrane vesicles treated with AlF_4^-. The figure is typical of 4 experiments.

3.10. All recombinant human SERCA3a–SERCA3f isoforms exhibit similar tryptic fragmentation profiles

Studies to investigate the intrinsic properties of the various recombinant human SERCA3 isoforms showed a similar reduced affinity towards Ca^{2+} compared to SERCA1. However, analysis of the catalytic cycle of SERCA3a, -3b, -3c and -3f isoforms revealed differences in the dephosphorylation of the *E*2P intermediate of these enzymes [21,30]. This led us to look for the tryptic fragmentation profiles of the SERCA3a–3f isoforms (Fig. 7) followed by Western blotting using the PL/IM430, N89 and isoform-specific anti-SERCA3a–3f antibodies. While anti-SERCA3a–3d and -3f antibodies [10,21,23] were available, a SERCA3e-specific antibody was lacking. Such an antibody was generated and characterized by testing its immunoreactivity on recombinant SERCA3a–3f proteins (Fig. 7A,B). The PL/IM430 antibody recognized all SERCA3 isoforms migrating at their predicted MW. The anti-SERCA3e-P2 antibody only recognized the recombinant SERCA3e isoform, and this signal was abolished by the P2 peptide used for immunization. Subpanels C–E of Fig. 7 show the effect of 50 μg/ml trypsin on stably transfected SERCA3a–3f isoforms. All isoforms exhibit similar ETF and LTF, as judged by: i) PL/IM430 (B/C and D/E fragments) (Fig. 7C) and ii) N89 (H fragment) (Fig. 7D) antibodies. Surprisingly, SERCA3b to SERCA3e isoforms sometimes appeared to be expressed as protein doublets recognized by the PL/IM430 (see also Fig. 8). In Fig. 7E, the isoform-specific anti-SERCA3a–3f antibodies (see Fig. 7A for their epitopes) were tested on intact and trypsinolyzed SERCA3a–SERCA3f proteins. The key observation was that major tryptic digests of about 31-, 36-, 34-, 36-, 37- and 35-kDa MW were recognized by the different anti-SERCA3a–3f antibodies, respectively. Compared with SERCA3a, additional 44, 30, 45, 53 and 34 aa long C-terminal ends are present in SERCA3b, -3c, -3d, -3e and -3f isoforms (see Figs. 7A and 8B). Therefore, the different C-terminal A fragments of SERCA3b–3f isoforms are coming from the same tryptic site as that giving rise to the A fragment of SERCA3a.

3.11. Only SERCA3b–SERCA3e isoforms exhibit an additional tryptic site at Arg^{1002}

In the protein doublets of the SERCA3b–3e isoforms recognized by PL/IM430 in trypsin-treated samples (Fig. 7C), the lower protein bands were not recognized by the anti-SERCA3b–3e antibodies (Fig. 7E). This observation pointed to an additional tryptic site in the C-terminal parts of these SERCA3 isoforms. In addition, the lower protein bands appeared to migrate as SERCA3a. This led us to postulate in favor of a common tryptic site giving rise to fragments with similar MW to that of SERCA3a. Fig. 8 establishes these data and identifies this tryptic site as Arg^{1002}. Through the technique of phosphorylated intermediate formation (autophosphorylation of Asp^{351}) of stably transfected SERCA3a–3f isoforms, Fig. 8A demonstrates the appearance of autophosphorylated doublets in the trypsin-treated SERCA3b–3e isoforms, which are also recognized by the PL/IM430 antibody. The doublets were particularly well visualized for the longer SERCA3b, -3d and -3e isoforms. Fig. 8B shows Arg^{1002}, which is only present in SERCA3b–3e isoforms (absent in SERCA3a and SERCA3f) as the

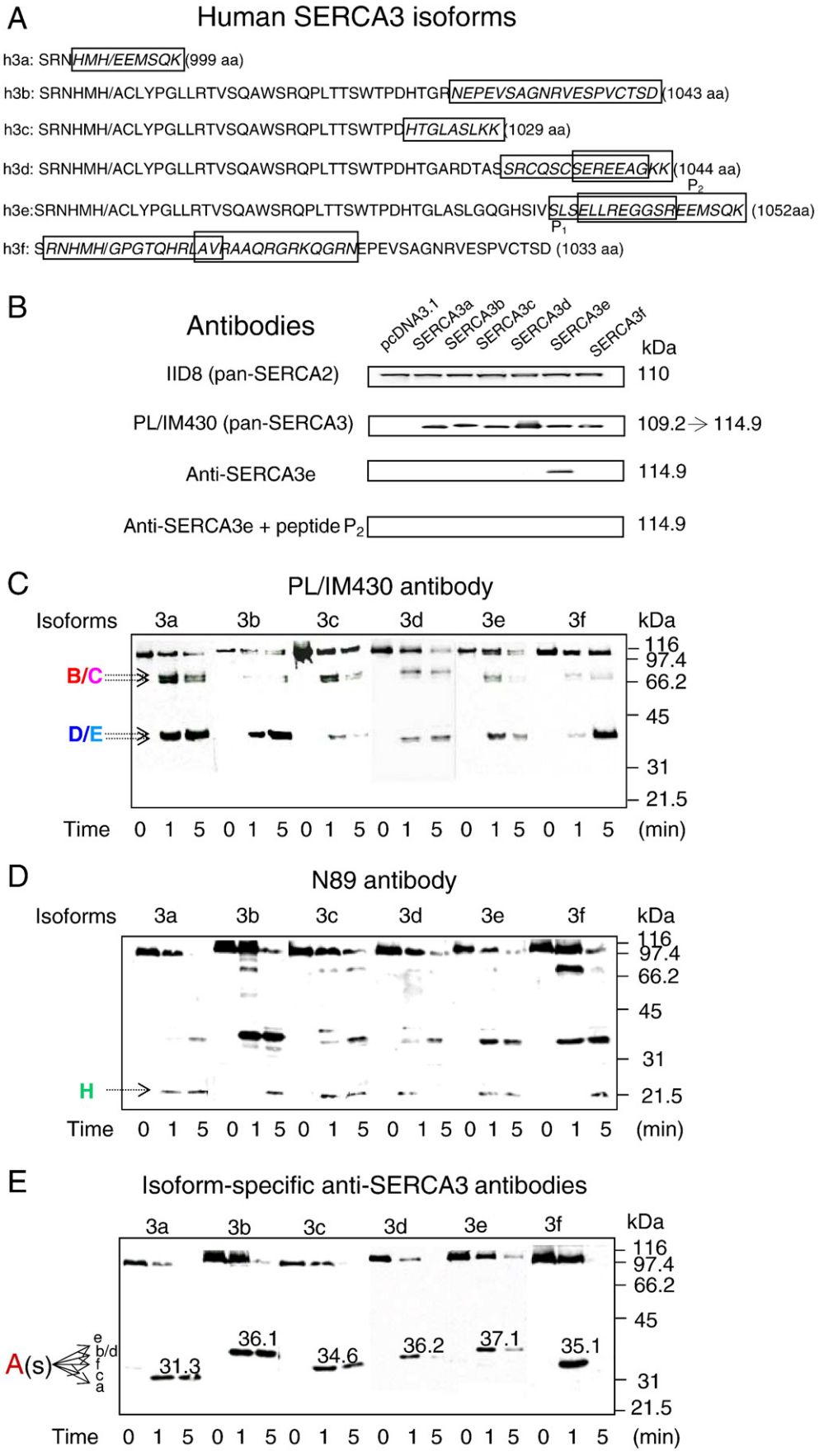
A
Human SERCA3 isoforms
h3a: SRNHMH/EEMSQK (999 aa)
h3b: SRNHMH/ACLYPGLLRTVSQAWSRQPLTTSWTPDHTGRNEPEVSAGNRVESPVCTSD (1043 aa)
h3c: SRNHMH/ACLYPGLLRTVSQAWSRQPLTTSWTPDHTGLASLKK (1029 aa)
h3d: SRNHMH/ACLYPGLLRTVSQAWSRQPLTTSWTPDHTGARDTASRCQSCSEREEAGKK (1044 aa)
P2
h3e:SRNHMH/ACLYPGLLRTVSQAWSRQPLTTSWTPDHTGLASLGQGHSIVSLSELLREGGSREEMSQK (1052aa)
P1
h3f: SRNHMH/GPGTQHRLAVRAAQRGRKQGRNEPEVSAGNRVESPVCTSD (1033 aa)
B
Antibodies
pcDNA3.1
SERCA3a
SERCA3b
SERCA3c
SERCA3d
SERCA3e
SERCA3f
kDa
IID8 (pan-SERCA2)
110
PL/IM430 (pan-SERCA3)
109.2 → 114.9
Anti-SERCA3e
114.9
Anti-SERCA3e + peptide P2
114.9
C
PL/IM430 antibody
Isoforms
3a
3b
3c
3d
3e
3f
kDa
116
97.4
66.2
45
31
21.5
B/C
D/E
Time
0 1 5 0 1 5 0 1 5 0 1 5 0 1 5 0 1 5
(min)
D
N89 antibody
Isoforms
3a
3b
3c
3d
3e
3f
kDa
116
97.4
66.2
45
31
21.5
H
Time
0 1 5 0 1 5 0 1 5 0 1 5 0 1 5 0 1 5
(min)
E
Isoform-specific anti-SERCA3 antibodies
3a
3b
3c
3d
3e
3f
kDa
116
97.4
66.2
45
31
21.5
A(s)
e
b/d
f
c
a
31.3
36.1
34.6
36.2
37.1
35.1
Time
0 1 5 0 1 5 0 1 5 0 1 5 0 1 5 0 1 5
(min)

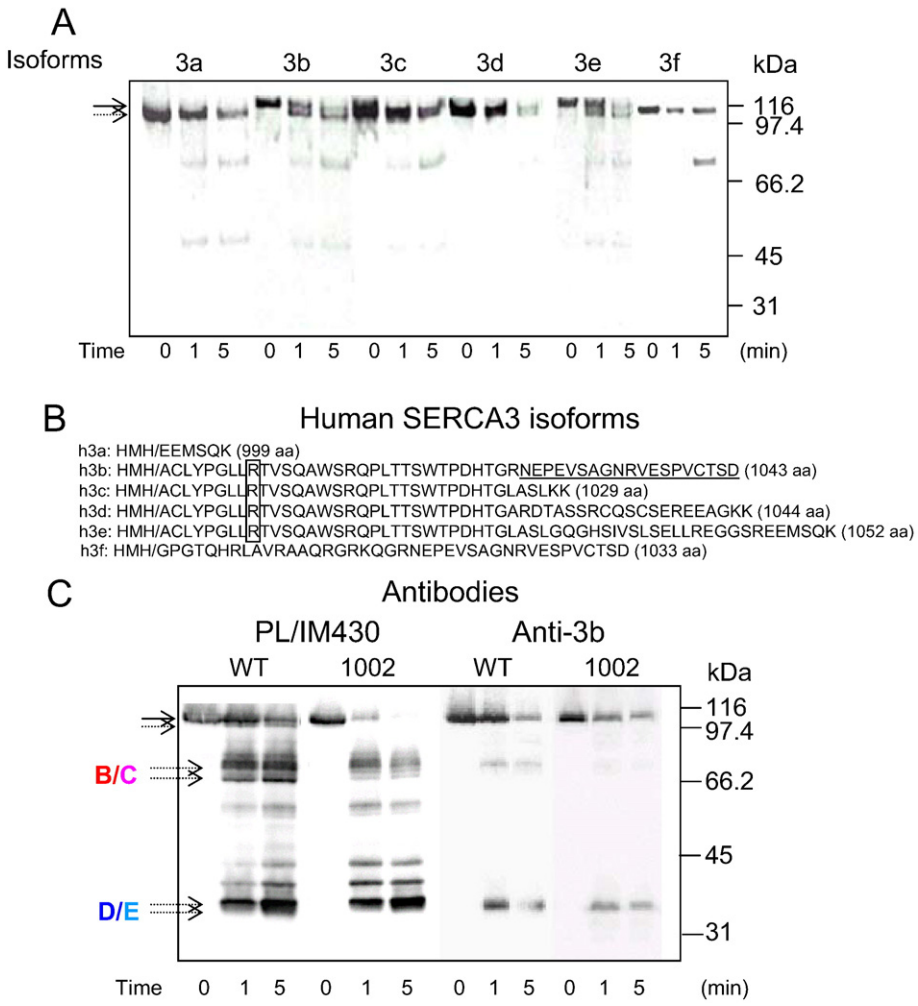

Fig. 8. SERCA3b–3e isoforms exhibit Arg^{1002} as an additional tryptic site. (A) Microsomal membranes isolated from HEK-293 cells stably transfected with SERCA3a–3f proteins were submitted to 50 μg/ml trypsin proteolysis at 4 °C for the time periods indicated. Intact and trypsinolyzed Ca^{2+} ATPases were then labeled with 0.05 μM [γ-^{32}P]ATP for 1 min, resolved by 7.5% acidic electrophoresis to preserve the aspartylphosphate intermediates of Ca^{2+} ATPases, blotted and autoradiographed [8,14,15]. This figure is typical of 3 experiments. (B) C-termini of human SERCA3 proteins. Slashes mark the first splice site. The sequence underlined represents the amino acid stretch used for SERCA3b immunization. The amino acids framed show the presence of Arg^{1002} in SERCA3b to -3e isoforms. (C) Recombinant SERCA3b protein was mutated at residue Arg^{1002} (R1002A) and transiently transfected in HEK-293 cells. Membrane vesicles were proteolyzed using 50 μg/ml trypsin for the time periods indicated. Wild Type (WT) and mutated SERCA3b proteins (R1002A) were then treated for Western blotting using PL/IM430 (left) and the isoform-specific anti-SERCA3b antibody (right). This figure is typical of 3 experiments.

potential tryptic site that gives rise to the lower bands of the doublets. Fig. 8C shows the effect of Arg^{1002} mutation (R1002A) on the tryptic fragmentation of one of the SERCA3b–3e isoforms, SERCA3b transiently transfected in HEK-293 cells. As expected, no protein doublet was detected upon trypsin proteolysis of the mutated SERCA3b protein, as shown by the PL/IM430 antibody. Reprobing the blots with the anti-SERCA3b antibody showed no differences in its recognition of a single protein band corresponding to either WT or R1002A mutant intact SERCA3b proteins. This is fully consistent with the lack of recognition of the SERCA3b truncated at Arg^{1002} by the antibody. The same study was performed on WT and mutant (R1002A) SERCA3e isoforms, which gave similar results as those obtained using SERCA3b (data not shown).

4. Discussion

Some twenty years ago we only knew the primary structure on several P-type ATPases. In that time tryptic digestion experiments were very useful tools to get information on the structure and conformational changes in these P-ATPases. Since 2000 [3] we know the crystal structure of SERCA1a and recently structures of Na^+, K^+-ATPase [31] and plant H^+-ATPase [32]. In addition, a large number of modeling studies have shown that the gross structure of the P-type ATPases is rather similar. As mentioned in the Introduction, in the intracellular domain of these transporters, A-, P- and N-subdomains can be recognized that undergo domain movements during the catalytic cycle. However, to answer the question of the physiological

Fig. 7. All SERCA3a–3f isoforms exhibit similar early and late tryptic profiles. (A and B) Generation of a novel SERCA3e-specific antibody. (A) C-terminal sequences of SERCA3a–3f proteins. Slashes indicate the splice sites. The framed sequences represent the peptides used for the different immunizations (Peptides P1 and P2 for SERCA3e). (B) Membrane proteins were isolated from HEK-293 cells stably transfected with empty vector pcDNA3.1 and SERCA3a–f cDNAs. Microsomes (10 μg) were used for Western blotting using the monoclonal pan-SERCA2 (IID8), the monoclonal pan-SERCA3 (PL/IM430) and the polyclonal anti-SERCA3e antibodies. To test the specificity of the anti-SERCA3e antibody, the blots were treated either in the absence or presence of 10 μM peptide (P2). The numbers indicate the calculated protein molecular masses in kDa. (C–E) SERCA3a–3e membrane protein vesicles were proteolyzed using 50 μg/ml trypsin and further treated for Western blottings using the PL/IM430 (C), N89 (D) and the various isoform-specific anti-SERCA3a–3f antibodies (E). The numbers on Fig. 7E indicate the calculated molecular masses of A fragments of the various isoforms, in kDa. This figure is typical of 6–7 experiments.

occurrence of conformational changes in the native membrane environment, other approaches have to be used. For this, again, changes in the pattern of tryptic proteolysis appeared to be a complementary technique. Accordingly, very recently, conformational fluctuations of SERCA1a in the native membrane environment have been described using proteolytic fragmentation approach with proteinase K or trypsin [18]. Here, by performing trypsinolysis of SERCA3 proteins in native human cell membranes, we described two, kinetically distinct, ETF and LTF profiles and identified some of the proposed T1–T5 tryptic sites (Fig. 1). T1–T2 would be a multi-tryptic site in the 638–728 region. T3–T4 would be a multi-tryptic site in the 290–396 region. T5 is at 198. In addition, a final tryptic site has been positioned at 1002 in SERCA3b–3e isoforms.

A study of *SERCA3* gene products is of interest for the following reasons at least: i) they are expressed in a number of cells and tissues [20,21,33,34]; ii) mutations in *SERCA3* gene have been described in patients with type II diabetes mellitus and squamous cell carcinoma [35,36]; iii) lack of SERCA3 altered endothelium- and epithelium-dependent relaxation in vascular smooth muscle [37,38]; iv) modulated SERCA3 expression has been documented during cell differentiation [39–43]; v) different roles of SERCA3b and -3f isoforms in cell function have been identified [44]; vi) a role of SERCA3 was very recently described in the mechanism of store-operated Ca^{2+} entry, a process that is very relevant in many cell functions [45–47].

In addition, as mentioned in the Introduction, early studies revealed a number of functional particularities of SERCA3a in the SERCA family. The first was its lower affinity towards Ca^{2+} than that observed for the SERCA1a, -2a and -2b proteins [7]. A second observation stemmed from studies using human platelets, which mainly express the SERCA3a isoform along with the SERCA2b isoform [48,49]. We showed that Tg and tBHQ inhibit Ca^{2+} uptake of mixed platelet membrane vesicles [50]. Intriguingly, SERCA3a was found to exhibit a lower sensitivity to Tg than SERCA2b [14]. Similar observation was recently made when using recombinant SERCA3a protein [51]. Conversely, SERCA3a was much more sensitive to tBHQ, than SERCA2b [15]. In addition, when we performed E~P formation and subsequent trypsinization of platelet membranes in the presence of either Tg or tBHQ (under experimental conditions that only detect the LTF), we observed that Tg slightly, while tBHQ almost totally inhibited the formation of the autophosphorylated 80-kDa fragment (G fragment in the present work) [8,14,15].

Here, using various anti-SERCA3 antibodies and limited trypsinolysis of SERCA3a (WT and mutants), we uncovered initial evidence for the ETF and LTF profiles of either human platelet SERCA3a protein, or transient and stable recombinant SERCA3a–3f isoforms coming from two SERCA3 conformational states.

The two distinct ETF and LTF profiles belong to SERCA3(s) as shown by their recognition with a variety of anti-SERCA3 antibodies. The two proteolytic patterns have been primarily dissociated on the basis of their different kinetics of trypsin proteolysis. Indeed, the late appearance of the longer G fragment in LTF cannot be explained with the progressive proteolytic profile of ETF. In addition, we showed that the mutation of Arg^{198}, that blocked the formation of the G and H fragments, only affected LTF without any effect on ETF. Last, ETF alone was found to be sensitive to Ca^{2+}, EGTA and AlF_4^-. In addition, based on the similarity of the Ca^{2+} and EGTA lanes, we can suggest that the SERCA3 population susceptible to T1–T4 (ETF) is in a close to E2 conformation.

We identified a number of tryptic sites involved in the ETF profile and a unique tryptic site involved in the LTF profile of the SERCA3 protein(s). For the more complex ETF, the direct involvement of Arg^{334}, Arg^{396} and Arg^{638} has been documented. We also tested the potential implication of Arg^{671}, Lys^{728} and $Lys^{712/713}$ in ETF, and found that these residues might account for the multi-tryptic site involved in the initial C-terminal fragmentation of SERCA3(s). In addition, two other tryptic sites were also suggested. First, based on the MWs of D and F fragments, we thought that Arg^{324} is the tryptic site that gives rise to the E fragment. Second, based on the results with R334A and R396A mutants, the ETF of which showed an additional fragment with higher MW than that of the F fragment, a trypsin attack at Arg^{290} could also be suggested. Arg^{365}, Arg^{403}, Arg^{613} and Arg^{686} were also mutated, but these mutations did not modify the ETF. For LTF, Arg^{198} has been definitely identified as major tryptic site. Lastly, thanks to the coupled use of the generation of autophosphorylated intermediates, and Western blottings, we were able to identify Arg^{1002} as an additional tryptic site common to SERCA3b to -3e isoforms.

In an attempt to gather further information about the ETF and LTF of SERCA3a, we studied the effect of SERCA inhibitors inducing the so-called *E2*(Tg) conformational state of SERCA1a. Here, by using recombinant SERCA3a protein, we found that both Tg and tBHQ slightly inhibited the ETF profile.

The ETF and LTF profiles were found not only for the SERCA3a isoform, but also for the other SERCA3b to -3f isoforms. We uncovered an additional tryptic site in the SERCA3b–3e isoforms as well, which is absent in SERCA3f. While the rationale for the diversity of SERCA3 isoforms remains to be understood, some differences have already been identified, including differences between SERCA3a, -3b, -3c and -3f in one of the steps of their catalytic cycles [21,30]. In addition, we recently observed that the SERCA3a, -3d and -3f isoforms also exhibit distinct locations in human heart. While SERCA3a was expressed in a uniform manner, SERCA3d and -3f were restricted to the nucleus and to the periphery of the cardiomyocyte, respectively [23]. The absence of Arg^{1002} in SERCA3f adds an additional difference to those published previously between the SERCA3 isoforms.

To conclude: 1) the present findings constitute evidence for co-expression of SERCA3 proteins in two conformational states in the native membrane environment. Can SERCA3 be a physiological prototype of SERCA in two major conformational states of SERCA1a? 2) Given the enigma of the lower Ca^{2+}-affinity of SERCA3 isoforms towards Ca^{2+} compared to those of SERCA1 and SERCA2 proteins, and the expression of SERCA3(s) in two conformational states including a close to E2 conformation, can these findings provide an initial explanation? 3) Such a particularity of SERCA3(s) would also explain the location of at least some of the isoforms in the subplasmalemmal area of cells, such as SERCA3f in the heart, where cellular Ca^{2+} concentration is higher. 4) The fluctuation of SERCA3 in the two major conformational states may also be needed for turning on/out a store-operated Ca^{2+} channel. Indeed, we recently observed the association of SERCA3 with the *ST*romal *I*nteraction *M*olecule 1 (STIM1) [47] the ER-resident Ca^{2+} binding protein that participates in various signaling complexes regulating the function of store-operated Ca^{2+} channels [for reviews see [52,53].

Acknowledgements

This work was supported by the INSERM (Institut National de la Santé et de la Recherche Médicale) and by the AFM (Association Française Contre les Myopathies) and by the Hungarian Academy of Sciences Grant OTKA T046814 (to T.K.). We thank Régis Bobe U. 689 INSERM for the help in the modification of the figures of the revised version of the manuscript.

Appendix A. Supplementary data

Supplementary data associated with this article can be found, in the online version, at doi:10.1016/j.bbamem.2008.12.004.

References

[1] S. Dally, R. Bredoux, E. Corvazier, J.P. Andersen, J.D. Clausen, L. Dode, M. Fanchaouy, P. Gélébart, V. Monceau, F. Del Monte, J.K. Gwathmey, R. Hajjar, C. Chaabane, R. Bobe, A. Raies, J. Enouf, Ca^{2+}-ATPases in non-failing and failing heart: evidence for a novel cardiac sarco/endoplasmic reticulum Ca^{2+} ATPase 2 isoform (SERCA2c), Biochem. J. 395 (2006) 249–258.

[2] R. Bobe, R. Bredoux, E. Corvazier, S. Dally, C. Chaabane, T. Kovàcs, J. Enouf, Sarco/endoplasmic reticulum Ca^{2+} ATPase (SERCA) isoforms: 1998: 5 proteins; 2005: 14 proteins, Curr. Top. Biochem. Res. 7 (2005) 1–15.

[3] C. Toyoshima, M. Nakasako, H. Nomura, H. Ogawa, Crystal structure of the calcium pump of sarcoplasmic reticulum at 2.6 A resolution, Nature 405 (2000) 647–655.

[4] C. Toyoshima, H. Nomura, Structural changes in the calcium pump accompanying the dissociation of calcium, Nature 418 (2002) 605–611.

[5] C. Toyoshima, T. Mizutani, Crystal structure of the calcium pump with a bound ATP analogue, Nature 430 (2004) 529–535.

[6] C. Olesen, M. Picard, A.M. Winther, C. Gyrup, J.P. Morth, C. Oxvig, J.V. Møller, P. Nissen, The structural basis of calcium transport by the calcium pump, Nature 450 (2007) 1036–1042.

[7] J. Lytton, M. Westlin, S.E. Burk, G.E. Shull, D.H. MacLennan, Functional comparisons between isoforms of the sarcoplasmic or endoplasmic reticulum family of calcium pumps, J. Biol. Chem. 267 (1992) 14483–14489.

[8] T. Kovàcs, E. Corvazier, B. Papp, C. Magnier, R. Bredoux, A. Enyedi, B. Sarkadi, J. Enouf, Controlled proteolysis of Ca^{2+}-ATPases in human platelet and non-muscle cell membrane vesicles. Evidence for a multi-sarco/endoplasmic reticulum Ca^{2+}-ATPase system, J. Biol. Chem. 269 (1994) 6177–6184.

[9] F. Wuytack, B. Papp, H. Verboomen, L. Raeymaekers, L. Dode, R. Bobe, J. Enouf, S. Bokkala, K.S. Authi, R. Casteels, A sarco/endoplasmic reticulum Ca^{2+} ATPase 3-type Ca^{2+} pump is expressed in platelets, in lymphoid cells, and in mast cells, J. Biol. Chem. 269 (1994) 1410–1416.

[10] T. Kovàcs, F. Felfoldi, B. Papp, K. Paszty, R. Bredoux, A. Enyedi, J. Enouf, All three splice variants of the human sarco/endoplasmic reticulum Ca^{2+} ATPase 3 gene are translated to proteins. A study of their co-expression in platelets and lymphoid cells, Biochem. J. 358 (2001) 559–568.

[11] C.P. Chandrasekera, J. Lytton, Inhibition of human SERCA3 by PL/IM430. Molecular analysis of the interaction, J. Biol. Chem. 278 (2003) 12482–12488.

[12] A. Enyedi, B. Sarkadi, Z. Foldes-Papp, S. Monostory, G. Gardos, Demonstration of two distinct calcium pumps in human platelet membrane vesicles, J. Biol. Chem. 261 (1986) 9558–9563.

[13] J. Enouf, A.-M. Lompré, R. Bredoux, N. Bourdeau, D. de la Bastie, S. Lévy-Tolèdano, Different sensitivity to trypsin of the human platelet plasma and intracellular membrane Ca^{2+} pumps, J. Biol. Chem. 263 (1988) 13922–13929.

[14] B. Papp, A. Enyedi, T. Kovàcs, B. Sarkadi, F. Wuytack, O. Thastrup, G. Gardos, R. Bredoux, S. Lévy-Tolèdano, J. Enouf, Demonstration of two forms of calcium pumps by thapsigargin inhibition and radioimmunoblotting in platelet membrane vesicles, J. Biol. Chem. 266 (1991) 14593–14596.

[15] B. Papp, A. Enyedi, K. Pàszty, T. Kovàcs, B. Sarkadi, G. Gàrdos, C. Magnier, F. Wuytack, J. Enouf, Simultaneous presence of two distinct endoplasmic-reticulum-type calcium-pump isoforms in human cells, Biochem. J. 288 (1992) 297–302.

[16] S. Danko, T. Daiho, K. Yamasaki, M. Kamidochi, H. Suzuki, C. Toyoshima, ADP-insensitive phosphoenzyme intermediate of sarcoplasmic reticulum Ca^{2+}-ATPase has a compact conformation resistant to proteinase K, V8 protease and trypsin, FEBS Lett. 489 (2001) 277–282.

[17] S. Danko, K. Yamasaki, T. Daiho, H. Suzuki, C. Toyoshima, Organization of cytoplasmic domains of sarcoplasmic reticulum Ca^{2+}-ATPase in E(1)P and E(1)ATP states: a limited proteolysis study, FEBS Lett. 505 (2001) 129–135.

[18] G. Inesi, D. Lewis, C. Toyoshima, A. Hirata, L. de Meis, Conformational fluctuations of the Ca^{2+}-ATPase in the native membrane environment: effects of pH, temperature, catalytic substrates, and thapsigargin, J. Biol. Chem. 283 (2008) 1189–1196.

[19] C. Lacabaratz-Porret, S. Launay, E. Corvazier, R. Bredoux, B. Papp, J. Enouf, Biogenesis of endoplasmic reticulum proteins involved in Ca^{2+} signalling during megakaryocytic differentiation: an in vitro study, Biochem. J. 350 (2000) 723–734.

[20] V. Martin, R. Bredoux, E. Corvazier, R. van Gorp, T. Kovàcs, P. Gélébart, J. Enouf, Three novel sarco/endoplasmic reticulum Ca^{2+} ATPase (SERCA) 3 isoforms, Expression, regulation and function of the members of the SERCA3 family, J. Biol. Chem. 277 (2002) 24442–24452.

[21] R. Bobe, R. Bredoux, E. Corvazier, J.P. Andersen, J.D. Clausen, L. Dode, T. Kovàcs, J. Enouf, Identification, expression, function and localization of a novel (sixth) isoform of the human Sarco/Endoplasmic Reticulum Ca^{2+} ATPase 3 (SERCA3) gene, J. Biol. Chem. 279 (2004) 24297–24306.

[22] A. Troullier, J.L. Girardet, Y. Dupont, Fluoroaluminate complexes are bifunctional analogues of phosphate in sarcoplasmic reticulum Ca^{2+}-ATPase, J. Biol. Chem. 267 (1992) 22821–22829.

[23] S. Dally, V. Monceau, E. Corvazier, R. Bredoux, A. Raies, R. Bobe, F. del Monte, J. Enouf, Compartmentalized expression of three novel sarco/endoplasmic reticulum Ca^{2+} ATPase 3 isoforms including the switch to ER stress, SERCA3f, in non-failing and failing human heart, Cell Calcium (2008) in press.

[24] W. Lesniak, N. Modyanov, M. Chiesi, Reversible inactivation of the sarcoplasmic reticulum Ca^{2+}-ATPase coupled to rearrangement of cytoplasmic protein domains as revealed by changes in trypsinization pattern, Biochemistry 33 (1994) 13678–13683.

[25] L. Dux, A. Martonosi, Ca^{2+}-ATPase membrane crystals in sarcoplasmic reticulum. The effect of trypsin digestion, J. Biol. Chem. 258 (1983) 10111–10115.

[26] Y. Imamura, K. Saito, M. Kawakita, Conformational change of Ca^{2+}, Mg^{2+}-adenosine triphosphatase of sarcoplasmic reticulum upon binding of Ca^{2+} and adenyl-5′-yl-imidodiphosphate as detected by trypsin sensitivity analysis, J. Biochem. 95 (1984) 1305–1313.

[27] J.P. Andersen, B. Vilsen, J.H. Collins, P.L. Jorgensen, Localization of E1–E2 conformational transitions of sarcoplasmic reticulum Ca^{2+}-ATPase by tryptic cleavage and hydrophobic labelling, J. Membr. Biol. 93 (1986) 85–92.

[28] B. Juul, H. Turc, M.-L. Durand, A. Gomez de Gracia, L. Denoroy, J.V. Møller, P. Champeil, M. le Maire, Do transmembrane segments in proteolyzed sarcoplasmic reticulum Ca^{2+}-ATPase retain their functional Ca^{2+} binding properties after removal of cytoplasmic fragments by proteinase K? J. Biol. Chem. 270 (1995) 20123–20134.

[29] P. Champeil, T. Menguy, S. Soulié, B. Juul, A. Gomez de Gracia, F. Rusconi, P. Falson, L. Denoroy, F. Henao, M. le Maire, J.V. Møller, Characterization of a protease-resistant domain of the cytosolic portion of sarcoplasmic reticulum Ca^{2+}-ATPase, J. Biol. Chem. 273 (1998) 6619–6631.

[30] L. Dode, B. Vilsen, K. Van Baelen, F. Wuytack, J.D. Clausen, J.P. Andersen, Dissection of the functional differences between sarco(endo)plasmic reticulum Ca^{2+}-ATPase (SERCA) 1 and 3 isoforms by steady-state and transient kinetic analyses, J. Biol. Chem. 277 (2002) 45579–45591.

[31] J.P. Morth, B.P. Pedersen, M.S. Toustrup-Jensen, T.L. Sorensen, J. Petersen, J.P. Andersen, B. Vilsen, P. Nissen, Crystal structure of the sodium–potassium pump, Nature 450 (2007) 1043–1049.

[32] B.P. Pedersen, M.J. Buch-Pedersen, J.P. Morth, M.G. Palmgren, P. Nissen, Crystal structure of the plasma membrane proton pump, Nature 450 (2007) 1111–1114.

[33] L. Dode, C. De Greef, I. Mountian, M. Attard, M.M. Town, R. Casteels, F. Wuytack, Structure of the human sarco/endoplasmic reticulum Ca^{2+}-ATPase 3 gene, promoter analysis and alternative splicing of the SERCA3 pre-mRNA, J. Biol. Chem. 273 (1998) 13982–13994.

[34] R. Bobe, R. Bredoux, E. Corvazier, C. Lacabaratz-Porret, V. Martin, T. Kovàcs, J. Enouf, How many Ca^{2+} ATPase isoforms are expressed in a cell type? A growing family of membrane proteins illustrated by studies in platelets, Platelets 16 (2005) 133–150.

[35] A. Varadi, L. Lebel, Y. Hashim, Z. Mehta, S.J. Ashcroft, R. Turner, Sequence variants of the sarco(endo)plasmic reticulum Ca^{2+}-transport ATPase 3 gene (SERCA3) in Caucasian type II diabetic patients (UK Prospective Diabetes Study 48), Diabetologia 42 (1999) 1240–1243.

[36] B. Korošec, D. Glavač, M. Volavšek, M. Ravnik-Glavač, Alterations in genes encoding sarcoplasmic–endoplasmic reticulum Ca^{2+} pumps in association with head and neck squamous cell carcinoma, Cancer Genet. Cytogenet. 181 (2008) 112–118.

[37] L.H. Liu, R.J. Paul, R.L. Sutliff, M.L. Miller, J.N. Lorenz, R.Y. Pun, J.J. Duffy, T. Doetschman, Y. Kimura, D.H. MacLennan, J.B. Hoying, G.E. Shull, Defective endothelium-dependent relaxation of vascular smooth muscle and endothelial cell Ca^{2+} signaling in mice lacking sarco(endo)plasmic reticulum Ca^{2+}-ATPase isoform 3, J. Biol. Chem. 272 (1997) 30538–30545.

[38] J. Kao, C.N. Fortner, L.H. Liu, G.E. Shull, R.J. Paul, Ablation of the SERCA3 gene alters epithelium-dependent relaxation in mouse tracheal smooth muscle, Am. J. Physiol. 277 (1999) L264–L270.

[39] S. Launay, M. Gianni, T. Kovàcs, R. Bredoux, A. Bruel, P. Gélébart, F. Zassadowski, C. Chomienne, J. Enouf, B. Papp, Lineage-specific modulation of calcium pump expression during myeloid differentiation, Blood 93 (1999) 4395–4405.

[40] P. Gélèbart, T. Kovàcs, J.P. Brouland, R. van Gorp, J. Grossmann, N. Rivard, Y. Panis, V. Martin, R. Bredoux, J. Enouf, B. Papp, Expression of endomembrane calcium pumps in colon and gastric cancer cells. Induction of SERCA3 expression during differentiation, J. Biol. Chem. 277 (2002) 26310–26320.

[41] S. Launay, M. Gianni, L. Diomede, L.M. Machesky, J. Enouf, B. Papp, Enhancement of ATRA-induced cell differentiation by inhibition of calcium accumulation into the endoplasmic reticulum: cross-talk between RARα and calcium-dependent signalling, Blood 101 (2003) 3220–3228.

[42] B. Papp, J.P. Brouland, P. Gélèbart, T. Kovàcs, C. Chomienne, C. Endoplasmic reticulum calcium transport ATPase expression during differentiation of colon cancer and leukaemia cells, Biochem. Biophys. Res. Commun. 322 (2004) 1223–1236.

[43] J.P. Brouland, P. Gélébart, T. Kovàcs, J. Enouf, J. Grossmann, B. Papp, The loss of SERCA3 expression is an early event during the multistep process of colon carcinogenesis, Am. J. Pathol. 167 (2005) 233–242.

[44] C. Chaabane, E. Corvazier, R. Bredoux, S. Dally, A. Raies, A. Villemain, E. Dupuy, J. Enouf, R. Bobe, Sarco/endoplasmic reticulum Ca^{2+} ATPase type 3 isoforms (SERCA3b and SERCA3f): distinct roles in cell adhesion and ER stress, Biochem. Biophys. Res. Commun. 345 (2006) 1377–1385.

[45] P.C. Redondo, G.M. Salido, J.A. Pariente, S.O. Sage, J.A. Rosado, SERCA2b and 3 play a regulatory role in store-operated calcium entry in human platelets, Cell Signal. 20 (2008) 337–346.

[46] P.C. Redondo, I. Jardin, J.J. Lopez, G.M. Salido, J.A. Rosado, Intracellular Ca^{2+} store depletion induces the formation of macromolecular complexes involving hTRPC1, hTRPC6, the type II IP_3 receptor and SERCA3 in human platelets, BBA Mol. Cell. Res. 1783 (2008) 1163–1176.

[47] J.J. Lopez, I. Jardin, R. Bobe, J.A. Pariente, J. Enouf, G.M. Salido, J.A. Rosado, STIM1 regulates acidic Ca^{2+} store refilling by interaction with SERCA3 in human platelets, Biochem. Pharmacol. 75 (2008) 2157–2164.

[48] J. Enouf, R. Bredoux, B. Papp, I. Djaffar, A.M. Lompré, N. Kieffer, O. Gayet, K. Clemetson, F. Wuytack, J.P. Rosa, Human platelets express the $SERCA_{2-b}$ isoform of Ca^{2+}-transport ATPase, Biochem. J. 286 (1992) 135–140.

[49] J. Enouf, R. Bobe, C. Lacabaratz-Porret, R. Bredoux, E. Corvazier, T. Kovàcs, B. Papp, The platelet Ca^{2+} transport ATPase system, Platelets 8 (1997) 5–13.

[50] B. Papp, K. Pàszty, T. Kovàcs, B. Sarkadi, G. Gàrdos, J. Enouf, A. Enyedi, Characterization of the inositol trisphosphate-sensitive and insensitive calcium stores by selective inhibition of the endoplasmic reticulum-type calcium pump isoforms in isolated platelet membrane vesicles, Cell Calcium 14 (1993) 531–538.

[51] L.L. Wootton, F. Michelangeli, The effects of the phenylalanine 256 to valine mutation on the sensitivity of sarcoplasmic/endoplasmic reticulum Ca^{2+} ATPase (SERCA) Ca^{2+} pump isoforms 1, 2, and 3 to thapsigargin and other inhibitors, J. Biol. Chem. 281 (2006) 6970–6976.

[52] P.F. Worley, W. Zeng, G.N. Huang, J.P. Yuan, J.Y. Kim, M.G. Lee, S. Muallem, TRPC channels as STIM1-regulated store-operated channels, Cell Calcium 42 (2007) 205–211.

[53] T. Hewavitharana, X. Deng, J. Soboloff, D.L. Gill, Role of STIM and Orai proteins in the store-operated calcium signaling pathway, Cell Calcium 42 (2007) 173–182.